Article

Not peer-reviewed version

Optical, Structural and Biological Characteristics of Rapid-Sintered Multichomatic Zirconia

Minja Miličić Lazić * , Nataša Jović Orsini , Miloš Lazarević , Vukoman Jokanović , Vanja Marjanović , Branimir N. Grgur

Posted Date: 22 August 2025

doi: 10.20944/preprints202508.1563.v1

Keywords: biomaterials; multichromatic zirconia; monolithic crown; cell proliferation; cell adhesion; fibroblasts; cielab; color space; XRD analysis

 doi:10.20944/preprints202508.1563.v1

Article

Optical, Structural and Biological Characteristics of Rapid-Sintered Multichomatic Zirconia

Minja Miličić Lazić [1,*], Nataša Jović Orsini [2], Miloš Lazarević [1], Vukoman Jokanović [2], Vanja Marjanović [1] and Branimir N. Grgur [3]

[1] Faculty of Dentistry, University of Belgrade, Serbia
[2] Vinča Institute of Nuclear Sciences - National Institute of the Republic of Serbia, University of Belgrade, P.O. Box 522, Belgrade, Serbia
[3] Faculty of Technology and Metallurgy University of Belgrade, Belgrade, Serbia
* Correspondence: minja.milicic@stomf.bg.ac.rs

Abstract

Background: To overcome the aesthetic limitations of dental monolithic zirconia restorations, multichromatic systems were developed to combine improved structural integrity with a natural shade gradient that mimics the optical properties of natural teeth. In response to the clinical demand for time-efficient, i.e. chairside fabrication of zirconia restorations, rapid sintering protocols became necessary to adjust clinical efficiency with material performance. This study addresses the challenges of rapid sintering protocol related to optical performance and phase transformation of the final restoration, and the zirconia-cell interaction. **Methods:** The influence of rapid sintering protocol on the color stability of the final dental restoration was evaluated by CIE L*a*b* color space. Phase transformation was assessed through X-ray diffraction analysis. Cellular behavior was evaluated by measuring wettability, materials surface energy and cells mitochondrial activity assay on human gingival fibroblasts. **Results:** Optical measurements demonstrated that the total color change of enamel layer of the polished samples were being higher than clinically acceptable values. Results of X-ray diffraction analysis, made for the fixed occupancy at $Z_{0.935}Y_{0.065}O_{0.984}$ revealed that rapid sintering caused a decrease in the cubic (C) phase and an increase in the total amount of tetragonal (T) phases. Additionally, a small amount of the monoclinic (M) phase is noticed. Although glazing as a surface finishing procedure resulted in increased hydrophility both polished and glazed surface-treated specimens showed statistically comparable cell adhesion and proliferation ($p>0.05$). **Conclusion:** Five times higher heating and cooling rates caused difficulty in reaching equilibrium, leading to changes in lattice parameters and the formation of the metastable T′ phase which could compromise aesthetic appearance of the final restoration.

Keywords: biomaterials; multichromatic zirconia; monolithic crown; cell proliferation; cell adhesion; fibroblasts; cielab; color space; XRD analysis

1. Introduction

Yttria-stabilized zirconia monolithic systems (ZrO_2–Y_2O_3) for all-ceramic restorations were initially introduced to reduce the risk of chipping and delamination in zirconia-based crowns veneered with porcelain. This single-piece restoration design not only minimizes the risk of structural failure but also offers enhanced control over sintering processes, reducing pore formation that could lead to long-term degradation [1,2]. However, the transition to monolithic zirconia restorations presented a unique challenge to clinicians due to their limited optical adaptability. Soon after widespread clinical use, the issue of natural appearance in monolithic zirconia restorations has been posed [3]. In order to compensate for aesthetic deficiency, various gradient technology (GT) procedures have been developed for the production of green zirconia components for simulating the shade gradient of human teeth.

 doi:10.20944/preprints202508.1563.v1

Multichromatic zirconia [4] was implemented by combining layers with diverse pigments to achieve a gradual shade transition from the cervical to the incisal part of the restoration, mimicking the natural tooth esthetics. The gradient color effect is created by adding a small amount of shading elements, like iron and rare earth elements, to the white zirconia base. The shading gradually increases from the incisal edge to the cervical area. The only distinction among the layers is in the pigment compositions, resulting in notable variations in shade while not affecting the translucency of the layers as anticipated [5]. Unlike conventional multilayer blocks, the multichromatic profile maintains consistent yttria concentrations across all layers. This uniform stabilizer oxide content also ensures similar flexural strength throughout the layers. Contrary to multichromatic, monochromatic multilayer zirconia is characterized by variation between tetragonal and cubic phase content, balancing translucency and strength to create a durable, visually pleasing, and harmonious material with a monolithic structure. This phase variation directly influences the material's microstructure, which, in turn, plays an important role in determining the optical properties.

The typical microstructure of dental yttrium-stabilized tetragonal zirconia (Y-TZP) consists predominantly of the tetragonal phase (S.G.$P4_2/nmc$), sintered to over 96% of its theoretical density [6]. The inclusion of alumina (Al_2O_3) in a small amount (at a concentration of 0.25 wt%) into the starting mix of powders enhances sinterability of doped zirconia, decreases porosity, and usually results in a reduced grain size (typically below 80 μm) of obtained ceramic [7,8].

Due to different structural and optical properties of tetragonal (S.G. $P4_2/nmc$) and cubic (S.G. $Fm\text{-}3m$) phases of zirconia, the optical behavior of the final restorations will be significantly affected by its phase composition [9–11]. The cubic phase exhibits a more stable crystal structure with less strain inside. This stability is due to its symmetrical crystal structure, where all three axes are of equal length ($a = b = c$), forming a perfect cubic lattice [12]. The inherent symmetry and thermodynamic stability of the cubic phase of zirconia make it less susceptible to changes under external conditions. In contrast, the tetragonal phase, with its asymmetrical unit cell, is more prone to distortion, strain, and phase transformation with yttria-substitution, but also with changes in processing. At the same time, the crystallite size of the tetragonal phase can be changed more easily. The structural characteristics of these two phases determine the optical behavior of zirconia-based materials. The tetragonal zirconia gives rise to birefringence, causing high opacity, while the cubic phase of zirconia with larger grains (influenced by 25-50 wt.% of cubic phase) contributes to higher light transmission and transparency [13]. The phase transition from tetragonal to cubic phase is expected at yttrium concentrations of approximately 10%, when the cubic phase becomes more stable. A fully stabilized cubic phase can only be achieved at concentrations greater than 8%, while at lower concentrations, the tetragonal phase is much more stable since a lower dopant concentration favors the stabilization of the tetragonal phase [14].

External factors such as temperature variations, mechanical stresses (present in dental applications), and different environmental influences (for example, humidity, exposure to corrosive chemicals, etc.) can significantly impact the stability of zirconia ceramics [10,11]. Given these considerations, this study primarily focuses on the effect of sintering protocols and surface finishing on zirconia stability.

The development of new sintering protocols focuses on addressing how sintering parameters affect microstructure, internal properties, and color reproduction in final restorations. Porosity and second-phase inclusions can hinder the natural transparency of a material, allowing gas entrapment in the structure during solidification, which can lead to light scattering and opacity.

Dental restorations are usually produced by soft milling of partially sintered materials or by hard milling of fully sintered materials. Hard milling involves a longer processing time and frequent tool replacements. Due to the exceptional hardness and flexural strength of fully sintered monolithic zirconia, hard milling is primarily used for manufacturing zirconia abutments and implants [15]. Hard machining can create internal microcracks into the structure of fully sintered 3Y-TZP (yttria-stabilized tetragonal zirconia polycrystal) blocks, leading to an increase in the monoclinic phase (S.G. $P2_1/c$)[16]. This phase transformation can result in surface microcracking, making the material more

 doi:10.20944/preprints202508.1563.v1

susceptible to low-temperature degradation (LTD).I n contrast, soft milling of partially sintered restorations needs a shorter milling time (approximately 15 minutes), opposite to hard milling, which requires at least three times longer time [17]. Therefore, the soft milling, as a cost-effective protocol, is expected to allow better control over mechanical properties of the final restoration.

However, an ongoing issue with the soft milling procedure is that the additional sintering step is time-consuming. To make zirconia crowns available as chair-side options, it became necessary to reevaluate sintering protocols. For that reason, a rapid sintering protocol is introduced and studied [18]. In addition to being time-effective, rapid sintering eliminates the need for temporization and reduces patient discomfort [19]. There was considerable controversy behind this concept during the previous period. First, the clinical relevance was not fully understood because it was unclear how rapid sintering affects the microstructure, structural parameters, phase composition, and consequently, the optical properties of the ceramic crowns.

With growing interest from the scientific community in this profound problem, and with color stability emerging as a critical esthetic parameter, the consensus on visual assessment of ceramic crowns centers on two primary thresholds for evaluating color variances [20]. It is crucial to underline that the 50:50% thresholds (perceptibility and acceptability) are traditionally highlighted, with the acceptability threshold (AT) carrying greater significance than the perceptibility threshold (PT). Achieving a color match between a zirconia crown and natural teeth below the 50:50% perceptibility threshold denotes a near-perfect match, where 50% of lay observers can perceive a color difference, while the other 50% cannot. As far as acceptability, the value of 50:50% refers to the situation where 50% of lay observers are in agreement. From a CIELab perspective, a ΔE (total color change) value of 1.2 corresponds to the 50:50% PT, whereas a ΔE value of 2.7 corresponds to the 50:50% acceptability threshold (AT) [20]. Color matches below the 50:50% PT are considered optimal. Yet, reaching such an imperceptible match can be challenging, expensive, and often unnecessary.

From a biological point of view, polishing, glazing, and pigment staining of zirconia all can yield surfaces that are highly biocompatible. The important factor for biological response is surface smoothness and chemistry: a smoother surface (whether achieved by polishing or glazing [21] promotes fibroblast adhesion, spreading, and proliferation, whereas rougher surfaces are less favorable. In vitro, gingival fibroblasts show attachment, high viability, and normal morphology on polished and glazed zirconia, even when pigments are present [21]. The goal is to form a well-finished zirconia (especially polished or appropriately glazed), which allows gingival tissues to integrate and maintain health, forming an epithelial seal and connective tissue adhesion with minimal inflammatory infiltrate.

The objective of this study was to determine the color change of a conventional and rapid-sintered multilayer zirconia. The research hypothesis was that there would not be differences between the optical parameters when comparing conventional and rapid-sintered zirconia. The additional aim of the study was to assess cellular biocompatibility and adhesion of polished and glazed surface of multichromatic zirconia.

2. Materials and Methods

2.1. Samples Preparation

The materials used in the present study were Multichromatic Katana STML (Kurary Noritake Dental, Tokyo, Japan) discs, A2 shade. Pre-sintered discs were cut by dry milling procedure, layer by layer (N=4), as specified in the manufacturer's instructions. Milling was performed using a dental milling machine VHF-K5. Milled samples were subjected to sintering following conventional (C) and rapid, i.e. speed (S) sintering methods. The evolution of temperature in time during these two protocols, T(t), was monitored automatically. According to it, the samples were separated into two groups:

a) Control group (samples denoted as CS)- obtained by the conventional sintering, when the heating and cooling was as followed:

 doi:10.20944/preprints202508.1563.v1

- Specimens were heated with a heating rate, ΔT/Δt= 10°C/min up to T = 1550 °C, followed by holding for 2 hours at that temperature, and then cooled for 153 min with a cooling rate 10°C/min to 20°C before removing from the furnace. Total sintering time was 7 h.

b) Experimental group (samples denoted as SS)- obtained by the speed sintering, were subjected to the followed protocols:

- Specimens were heated with a heating rate 50°C/min up to 1400°C, then with 4°C/min up to temperature 1500 °C, and the last 16 min with 10°C/min up to 1560 °C. The cooling was with a cooling rate 50 °C/min down to 800 °C, dwelling for 5 min, when the specimens were removed from the furnance and left to cool down to room temperature(for approximately 15 min). Total sintering time was 90 min.

After sintering, the final dimensions of the samples were 10 x 13 x 1mm. Additionally, the sintered samples were subjected to surface characterization treatment. Half of them were polished, and the other half were glazed.

a) Polished specimens - underwent dry polishing performed with SagemaxNexxZr Shine Kit-diamond rubber polishers(rubber polishers for pre-polishing and high-gloss polish with diamond paste).

b) Glazed specimens- underwent a transparent aluminosilicate glass deposition on a surface.

2.2. Color Measurements

Color measurements were performed using a digital reflectance spectrophotometer Datacolor SF300 in the 400–700 nm range under the D65 standard illuminant using the 10° standard observer. For each specimen, measurements were conducted four times, and their average was recorded. On the basis of measured CIE color coordinates (lightness, L*; red-green value, a*; and yellow-blue value, b*), color difference (ΔE*) was determined as:

$$\Delta E^* = \sqrt{\left(\Delta a^*\right)^2 + \left(\Delta b^*\right)^2 + \left(\Delta L^*\right)^2}$$

where ΔL* - is the color lightness difference between analyzed specimens, Δa*- red/green difference between analyzed specimens and Δb* - yellow/blue difference between analyzed specimens [22].

2.3. X-Ray Diffraction (XRD)

X-ray diffraction experiment was carried out on a *Rigaku SmartLab* diffractometer (Rigaku Co.) equipped with Cu Kα,β sources of radiation (30 mA, 40 kV) and a Dtex 250 detector. XRD patterns of the samples were collected in a Bragg-Brentano geometry, in the range of 10-90° 2θ with the step size 0.02° and a counting rate 1°/min. The measurements were made on a surface of the sintered samples. To investigate the effect of sintering protocol on a possible phase change of samples, the collected X-ray diffraction data were analyzed by the Rietveld method. Rietveld refinement was performed using integrated PDXL2 software incorporated into the *SmartLab Studio* package. Peak profiles were fitted using split pseudo-Voigt function. The presence of phases: the tetragonal (S.G.$P4_2/nmc$) and the cubic (S.G. Fm-$3m$) yttria-doped zirconia were introduced in the initial structural model applying Auto Search (suggested the ISCD cards with the best agreeing data). The microstructural analysis, based on the Halder-Wagner method [23] resulted in the estimated the crystallite size, D_{xrd}, and lattice strain, ε, values.

2.4. Physical Analysis-Contact Angle Measurements

Surface wettability measurement was conducted under the room temperature (22.5±0.2 °C) conditions. Samples were set onto measurement bench and a standardized volume of liquid (2µl of destilled water, diiodmethane and ethylene glycol) was applied to the sample's surface using a micropipette (Finnpipette, Thermo Fisher, Helsinki, Finland), at a distance of 4 mm and angle of 90°. Contact angles (θ) were measured 1 s after the liquid achieved contact with the substrate surface. The

 doi:10.20944/preprints202508.1563.v1

setup for the analyzer consists of Canon 77D camera, equipped with Canon ultrasonic microlens of 100 mm (Tokyo, Japan) and position stand. Data were analyzed using ImageJ contact angle software plugin (version 1.5t, National Institutes of Health, LOCI, University of Wisconsin, Madison, Wisconsin, USA). Additionally, surface free energy of the polished and glazed samples was calculated using the Owens-Wendt-Kaelble approach, using web-based SEC software [24].

2.5. Biocompatibility Evaluation on Human Gingival Fibroblasts

Human gingival fibroblasts (hGFs) were isolated from gingival tissues obtained with written consent from two healthy donors (n =2) during tooth extraction. Gingival tissues were minced into approximately 1 mm^3 fragments and subjected to the outgrowth method of cell cultivation. The minced tissue was placed in 25 cm^2 culture flasks with the complete growth medium (DMEM/F12 supplemented with 10% FBS and 1% ABAM, all from Gibco, ThermoFisher (Waltham, MA, USA) and incubated at 37 °C in a humidified 5% CO_2atmosphere. The cells obtained after the third passage were used in the study.

For biocompatibility testing, MTT and lactate dehydrogenase (LDH) tests were performed. The zirconia discs (polished and glazed) were placed onto 24-well plates; 2 × 10^4 cells were seeded onto discs and incubated in freshly prepared growth medium at 37 °C in a humidified 5% CO_2 atmosphere for 24 h. This medium was then used for the LDH assay which was performed using the manufacturer's, CyQUANT™ LDH Cytotoxicity Assay guidelines (Catalog no. C20300, ThermoFisher, Waltham, MA, USA). For the MTT assay, disks with attached cells were transferred to a new 24-well plate, and 500 µL of solution containing 3-(4,5-dimethylthiazol-2-yl)-2,5 diphenyltetrazolium bromide (MTT, 0.5 mg/mL) (Sigma-Aldrich, St. Louis, MO, USA) was added to each well and incubated for 4h. The supernatant was then discarded; 500 µL of dimethyl sulfoxide (Sigma-Aldrich, St. Louis, MO, USA) was added to each well; and the plate was placed on a shaker for 20 min, at 250 rpm, in the dark, at 37 °C. The extracted colored solutions from 24-well plates were transferred into a new 96-well plate. The optical density was measured at 570 nm using a microplate reader RT-2100c (Rayto, Shenzhen, China). The percentage of cells viability was calculated as the difference from the control group (cells seeded on plastic), using the formula(OD (sample)- OD (Blank)/ OD (control)- OD (Blank)) ×100. There were three iterations of the experiment. There were three iterations of the experiment.

Cell adhesion assay was done to assess the potential of cell attachment to materials. Cells (1 × 10^4) were seeded onto materials and cultured in an incubator with 5% CO_2at 37 °C for 24 hours. Following the incubation period, non-adherent cells were quantified utilizing a hemocytometer. As a control, an equivalent number of cells was seeded in unoccupied 24-well culture plates. The adhesion rate (%) is calculated using the formula (number of seeded cells − non-adhered cells)/(number of seeded cells) × 100. This formula (Cai et al. 2018)was employed to determine the number of non-adherent cells following a 24-hour treatment. The experiment was conducted in three iterations.

3. Results

3.1. Optical Properties

The mean values of CIELab color coordinates after different sintering protocols are given in Table 1.

3.1.1. Differences in Total Color Change of Speed Sintered Samples

Table 1 show the color change, E* of speed sintered Katana specimens (SS), which were polished or glazed after sintering. The polished Katana specimens showed the highest change in color. ΔE*of samples in all layers were above the perceptibility threshold (PT) (ΔE*>1.2). Value detected only in enamel layer (EL) was higher than clinically acceptable (ΔE*>2.7). It was also observed that the EL of

 doi:10.20944/preprints202508.1563.v1

speed sintered and polished Katana specimen became reddish (a*+), and yellowish (b*+). At the same time, ΔE change was highly influenced by Δb* within the all layers of Katana specimens.

3.1.2. Differences in L* and C* Values

For polished Katana sampes, enamel layer (EL) exhibited higher color change and the lightness difference (ΔL), contributed the most to color change of this sample. This value slightly exceeded the AT for lightness difference (ΔL*>2.44) [25]. Upon evaluating changes in lightness, all polished specimens showed decrease in the ΔL from enamel layer (EL) to the body layer (BL). Similar results were observed for glazed samples.

Regarding changes in chroma, none of the tested samples exhibited values higher than the AT ones (ΔC*<3.15) [25]. Nevertheless, it should be noticed that the change in chroma was the main factor influencing the color variation of the BL of glazed Katana.

Table 1. Color coordinates for SS Katana specimens.

	Layer	Δ*E**	Δ*L**	ΔC*	ΔH*	Δa*	Δb*
Polished	Enamel	3.013	2.453	1.621	-0.659	0.444	1.692
	Transition 1	1.643	0.511	1.544	-0.227	0.095	1.558
	Transition 2	1.514	0.362	1.482	-0.298	0.245	1.446
	Body	1.496	0.600	1.337	-0.298	0.326	1.331
Glazed	Enamel	2.580	1.593	1.888	-0.747	0.345	2.000
	Transition 1	1.528	0.168	1.466	-0.398	0.196	1.506
	Transition 2	1.925	-0.247	1.683	-0.488	0.263	1.832
	Body	2.196	-0.925	2.256	-0.274	0.244	2.259

3.2. The Crystal Structure of Sintered Katana STML Samples

Experimentally collected XRD data of polished and glazed Katana STML samples, sintered following conventional protocol (CS) or speed sintering route (SS), are shown in Figure 1. Given the fact that only EL of Katana polished samples showed changes in color parameters beyond AT values, a subsequent analysis of their phase structure was conducted. Two low intensity peaks labeled by asterisks in the sample SS-Katana STML probably belong to a small amount of the monoclinic phase ($P2_1/c$). The crystal structure refinement of the conventionally, CS- and speed sintered, SS- Katana, along with the phase quantification, were performed using the obtained XRD data and the PDXL software. The refinement was done tested different structural models and keeping the stoichiometry of the samples at $Zr_{0.935}Y_{0.065}O_{0.984}$. Among the most plausible approaches was singled out the model which include the presence of two phases for the CS-Katana STML and three phases for the SS-Katana STML. The most competitive models for the CS-Katana were the one in which coexist two tetragonal phases versus the model with one tetragonal (S.G. $P4_2/nmc$) and one cubic (S.G. Fm-3m) phase. Since the better agreement for the CS-Katana gave the second model, the results of refinement using one tetragonal (T) and one cubic (C) phase are given below. For the sample SS-Katana, additional tetragonal phase (T1) was introduced during refinement. Figure 2 shows the results of Rietveld refinement for the samples CS- and SS-Katana. Table 2 list the structural parameters, as well as the crystallite size, D_{XRD} and the lattice strain, ε, estimated by the Halder-Wagner method [23]. The results of the quantitative analysis (i.e., estimated phase composition) based on the RIR method (weight %), are also given in Table 2.

 doi:10.20944/preprints202508.1563.v1

Table 2. The results of Rietveld refinement for the EL samples of CS- and SS-Katana.

	The heating rate (°C/min)	Phase	Lattice parameters (Å)	Phase fraction (wt.%)	Tetragonality, $c/\sqrt{2}\ a$	Crystallite size, D_{XRD} (nm)	Lattice strain, ε (%)
CS-Katana	10	Tetragonal (S.G. *P*4₂/*nmc*)	$a = b = 3.633(7)$, $c = 5.124(8)$	54(8)	0.997	17 ± 2	0
		Cubic (S.G. *Fm*-3*m*)	$a = b = c = 5.137(7)$	46(8)			
SS-Katana	50	Tetragonal (T)	$a = b = 3.627(7)$, $c = 5.157(8)$	49(3)	1.005	19 ± 2	0.2(2)
		Tetragonal (T1)	$a = b = 3.615(7)$, $c = 5.168(8)$	27(2)	1.011		
		Cubic (C)	$a = b = c = 5.189(9)$	24(4)			

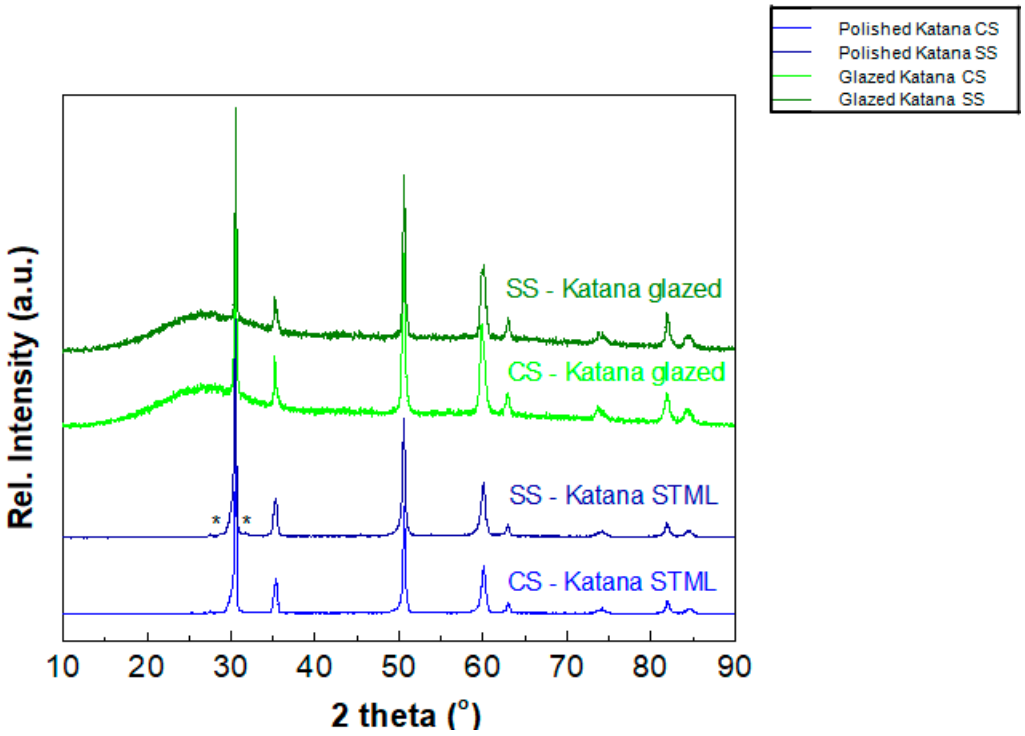

Figure 1. XRD data of glazed and polished EL of Katana STML, conventionally, CS- and speed sintered, SS-.

 doi:10.20944/preprints202508.1563.v1

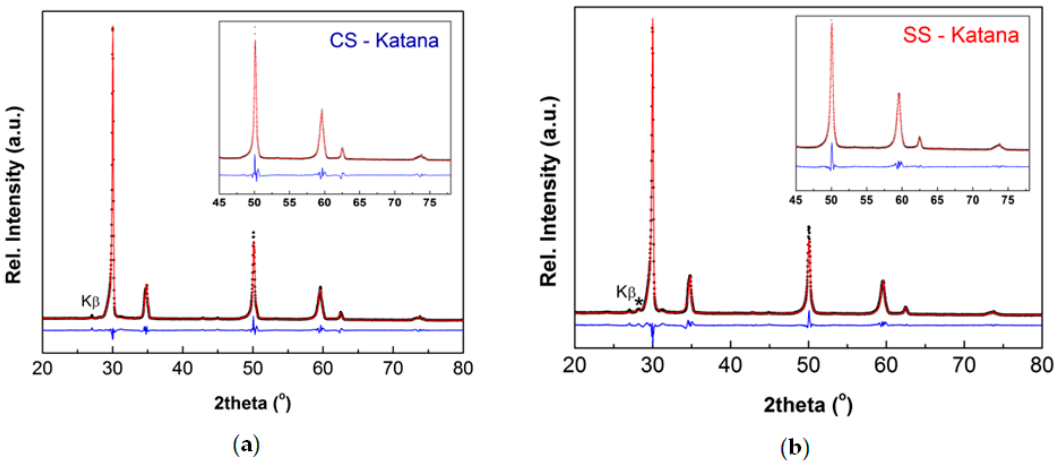

Figure 2. Refined XRD data of **(a)** conventionally (CS-) and **(b)** speed sintered (SS-) Katana STML.

3.3. Contact Angle Measurements

The water wetting angle measurements of polished and glazed zirconia samples showed that both surfaces presented a hydrophilic behavior (Table 3). Still, for glazed zirconia lower values of contact angle were observed in comparison to polished zirconia.

Table 3. Descriptive statistics of contact angle measurements (Mean ± St.dev).

Liquid	Sample	
	Polished	Glazed
Water	45.12±12	32.26±1.80
Ethylene glycol	50.06±3.12	28.06±1.45
Diiodmethane	42.55±1.98	35.50±2.20

Calculated surface energy value for glazed was 67.2 mJ/m^2, and for polished 59.4 mJ/m^2.

3.4. Comparable Cell Viability and Attachment on Polished and Glazed Zirconia Surfaces

After 24 hours of cell exposure to the polished and glazed zirconia, mitochondrial activity and LDH levels, which correspond to cell viability, were similar ($p>0.05$). The cell attachment exhibited comparable results for both polished and glazed materials ($p>0.05$) (Figure 3).

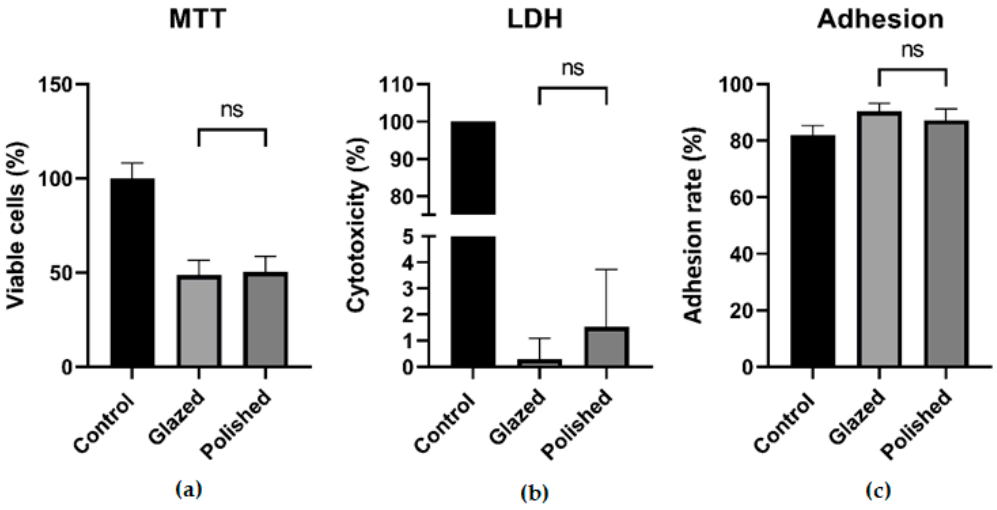

Figure 3. MTT (a), LDH (b), and Cell Adhesion (c) assays of hGFs seeded onto polished and glazed zirconia disks; ns- not significant.

 doi:10.20944/preprints202508.1563.v1

4. Discussion

This study verified color stability of each layer of multichromatic blocks independently. Obtained results offered partial evidence against the research hypothesis, indicating that speed sintering protocol has an effect on the optical properties of Katana zirconia, but only in the enamel layer.

Currently available data regarding changes in optical parameters in rapid sintering ceramics are mainly focused on research concerning changes in translucency [19,26–28]. Studies revealed that sintering speed did not affect the translucency of Katana STML zirconia [28]. According to recent research, speed-sintered zirconia can show a slight increase in translucency and lightness, but these changes may not be perceptible to the human eye in a clinical context. These findings highlight that obtained optical adjustments are often subtle and primarily noted in specific layers of multilayered zirconia rather than uniformly across the material. Our findings suggest that those changes were notable just in the enamel layer of Katana.

The obtained results were subsequently compared to the clinical threshold values previously reported in clinical research [29] . As per literature data, the perceptibility threshold was established at 1.2, while the threshold for acceptability was set to 2.7 [25]. This comparison was essential to contextualize our findings within clinically relevant parameters. The range of ΔE of the polished Katana specimens was between 1.5 and 3.0, meaning that obtained values were higher than ΔE PT (>1.2) in the case of all layers. However, in terms of the acceptability threshold, only the enamel layer exhibited values exceeding the ΔE AT (>2.7). Analyzing the results in the group of glazed samples from the aspect of PT, results were similar to the polished samples, as ΔE values ranged between 1.5 and 2.5 and thus were higher than ΔE PT in all layers. The color difference was not observed in the mean of the acceptability threshold, as all the results were lower than 2.7.

The results also show that the polished samples exhibited a more significant change in lightness compared to the glazed samples. This outcome is expected, as studies [30,31] examining the difference in lightness between polished and glazed crowns agree that, under the same conditions, polished crowns appear brighter. This is because the polishing process creates smooth, glossy surfaces that enhance specular light reflection. Additionally, it has been reported that diamond abrasive pastes used for polishing can impart a luster to the surface. Glazing creates a surface texture with dots and ridges that represents areas of highest convexity, where light is more likely to reflect. Conversely, pits and concavities on the surface are areas where light rays are more likely to be absorbed.

Taking into account phase quantification of Katana STML samples, literature data suggest variations in the phase composition depending on the sintering protocol. Also, the phase composition depends on the mol.% of Y_2O_3 that stabilized tetragonal zirconia polycrystal. According to some authors, the cubic phase in Katana STML can range from 55 wt.% to 70 wt.% [32]. We are aware that the XRD technique is not sensitive enough to detect the cubic-tetragonal phase transition in zirconia ceramics, primarily because oxygen has a relatively low atomic scattering factor. Similarly, electron diffraction and Raman scattering are not effective at measuring oxygen displacement, which is a key factor for quantitatively analyzing the cubic-tetragonal phase transition using an order parameter [33–35]. Here, additional difficulty arises from the nanoparticulate nature of the CS- and SS-Katana samples (visible by broadened reflections). According to the phase diagram of zirconia [36], phase transition from tetragonal to cubic phase can occur by increasing yttria content at around 10% [Solid State Ionic] or by increasing cooling rate. Results of our study, made for the fixed occupancy at $Zr_{0.935}Y_{0.065}O_{0.984}$ and presented in Table 2, revealed that speed sintering caused a decrease in the cubic (C) phase and an increase in the total amount of tetragonal (T_{tot}) phases. Additionally, a small amount of the monoclinic (M) phase is noticed (Figure 2). According to the literature data [37], two possible reasons can explain the presence of M-phase. Primarily, higher heating rates may not provide sufficient time for the complete transformation of the monoclinic to tetragonal phase, resulting in residual monoclinic phase. From the clinical point of view, this can increase the susceptibility to low-temperature degradation (LTD), compromising the longevity of the restoration. Secondarily, the

 doi:10.20944/preprints202508.1563.v1

effect of higher cooling rates may compromise the stability of the tetragonal phase, potentially leading to unwanted monoclinic transformation.

Correspondingly, in a study where Katana STML was sintered at 1560 °C for a holding time of 7 min, a decrease in cubic phase was noted, together with an increase in the tetragonal phase with elevated tetragonality [38]. Reports from other studies also indicate that when dental zirconia with less than 7.5 mol% yttria is rapidly cooled from temperatures above 1425 °C, it may form a metastable tetragonal phase instead of the cubic phase [39]. In our study, when both the heating and cooling rates were five times higher for the speed-sintered samples compared to the conventional ones, the appearance of the metastable tetragonal phase (T1) was also noticed. In addition, the heating rate during sintering changed the lattice parameters of all phases (see Table 2). The tetragonality value, $c/\sqrt{2}a$, of theT1-phase is higher than 1, indicating that this phase is with the lower yttrium region [40]. This can be due to the difficulty to reach the equilibrium state during speed sintering. Rapid thermal expansion causing the internal thermal stress doesn't allow enough time for the grain boundaries to equilibrate. The low yttrium region can be selectivity transformed into monoclinic (M) phase. Indeed, two peaks labeled by asterisk in Figure 2 were signed to the M-phase. At the same time, by increasing the heating and cooling rate, $\Delta T/\Delta t$, during the sintering process, the crystallite size, D_{XRD}, stayed almost unchanged, while the lattice strain, ε increased in the speed-sintered sample (SS- Katana STML) (here ε mostly arise from dislocations inside the crystal structure) [33]. The phase fraction (weight%) of cubic (C-) and tetragonal (T-) phases, calculated by the RIR method, is given in Table 2, too.

Thanks to the fact that polycrystalline zirconia contains a predominantly crystal structure characterized by smaller grains and more boundaries per surface compared to glass-ceramic materials, this favors the possibility of final polishing instead of only glazing. The influence of different surface finishing on bacterial adhesion and colonization is well-documented. Materials with surface ability to bind water molecules can influece various processes, incuding enhanced microbial attachment to their surface. As reported in previous research [41] hydrophilic surfaces may also help to reduce antagonist wear. Improved lubrication during contact reduce friction and wear between antagonistic surfaces.

However, the literature lacks evidence about differences in cellular adhesion on polished versus glazed zirconia. In the gingival area, the surface wettability of ZrO2 plays an important role in its soft-tissue integration via modulation protein adsorption and properties of hGF [42]. By tuning zirconia (via polishing, glazing, etc.), its hydrophilicity could be changed, influencing hGF response[42,43]. The data suggests that the most favorable contact angle value for cell adhesion and protein adsorption is around 40º, which characterizes moderate hydrophilicity [44,45]. Generally, smoother and more hydrophilic zirconia surfaces promote superior fibroblast adhesion and proliferation. In a recent study, investigation of polished versus glazed zirconia yields comparable cell outcomes —both finishes are smooth enough that their minor wettability differences do not appreciably alter HGF adhesion/proliferation [46]. This is in line with our study, as significant differences in cellular adhesion and viability were not detected. Although the polished and glazed surfaces did not show differences in promoting fibroblast viability and attachment, further research is needed to better understand this interaction and confirm the results. There is much room for further investigation and optimization of the surface characteristics of ZrO2 ceramics to enhance biological interactions with hGFs.

5. Conclusions

- The sample color measurements in this study showed that the rapid-sintered Katana STML had higher lightness compared to the conventionally sintered sample in the area corresponding to the incisal part of the crown.
- XRD analysis of multichromatic zirconia revealed appearance of the yttria-lean T1-phase with high tetragonality in the speed sintered zirconia samples.

 doi:10.20944/preprints202508.1563.v1

- Glazing as a surface finishing procedure increased hydrophilicity and surface energy values.
- Both polished and glazed zirconia demonstrated comparable cell viability and attachment.

Consequently, the properties of dental zirconia achieved via rapid sintering were not identical to those of zirconia processed using traditional sintering protocols. In conclusion, the changes in the sintering protocol could sacrifice the total color change of the material, and thus compromise esthetics appearance of the final restoration.

Author Contributions: Conceptualization, M.M.L., and N.J.O.; methodology, M.M.L., N.J.O., M.L.; software, M.M.L., N.J.O. and M.L.; validation, V.J. and B.N.G.; formal analysis, V.M.; investigation, M.M.L. and V.M.; resources, M.M.L. and V.J.; data curation, M.M.L. and N.J.O.; writing—original draft preparation, M.M.L. and N.J.O; writing—review and editing, M.M.L., N.J.O., and B.N.G.; visualization, V.M. and M.L.; supervision, V.J. and B.N.G.; project administration, M.M.L.; funding acquisition, M.M.L. All authors have read and agreed to the published version of the manuscript.

Funding: This research was conducted without external funding.

Institutional Review Board Statement: This study was conducted in accordance with the Declaration of Helsinki and approved by the Institutional Review Board of the Faculty of Dental Medicine, University of Belgrade (protocol code 36/7, approval date: 11 March 2020).

Data Availability Statement: The original contributions presented in this study are included in the article. Further inquiries can be directed to the corresponding author.

Acknowledgments: We sincerely thank Maja Radetić, from Department of Textile Engineering from Faculty of Technology and Metallurgy University of Belgrade, Serbia for her valuable assistance with the color measurements of the samples.

Conflicts of Interest: The authors declare no conflicts of interest.

References

1. Park, M.-G. Effect of Low-Temperature Degradation Treatment on Hardness, Color, and Translucency of Single Layers of Multilayered Zirconia. *The Journal of Prosthetic Dentistry* **2023**, doi:10.1016/j.prosdent.2023.01.023.
2. Kohorst, P.; Borchers, L.; Strempel, J.; Stiesch, M.; Hassel, T.; Bach, F.-W.; Hübsch, C. Low-Temperature Degradation of Different Zirconia Ceramics for Dental Applications. *Acta Biomaterialia* **2012**, *8*, 1213–1220, doi:10.1016/j.actbio.2011.11.016.
3. Manziuc, M.; Gasparik, C.; Negucioiu, M.; Constantiniuc, M.; Alexandru, B.; Vlas, I.; Dudea, D. Optical Properties of Translucent Zirconia: A Review of the Literature. *The EuroBiotech Journal* **2019**, *3*, 45–51, doi:10.2478/ebtj-2019-0005.
4. Benalcázar Jalkh, E.; Bergamo, E.; Campos, T.; Coelho, P.; Sailer, I.; Yamaguchi, S.; Alves, L.; Witek, L.; Tebcherani, S.; Bonfante, E. A Narrative Review on Polycrystalline Ceramics for Dental Applications and Proposed Update of a Classification System. *Materials* **2023**, *16*, 7541, doi:10.3390/ma16247541.
5. Kolakarnprasert, N.; Kaizer, M.R.; Kim, D.; Zhang, Y. New Multi-Layered Zirconias: Composition, Microstructure and Translucency. *Dent Mater* **2019**, *35*, 797–806, doi:10.1016/j.dental.2019.02.017.
6. Cesar, P.F.; Miranda, R.B. de P.; Santos, K.F.; Scherrer, S.S.; Zhang, Y. Recent Advances in Dental Zirconia: 15 Years of Material and Processing Evolution. *Dental Materials* **2024**, *40*, 824–836, doi:10.1016/j.dental.2024.02.026.
7. Alghazzawi, T.F. The Effect of Extended Aging on the Optical Properties of Different Zirconia Materials. *J Prosthodont Res* **2017**, *61*, 305–314, doi:10.1016/j.jpor.2016.11.002.
8. Zhang, Y. Making Yttria-Stabilized Tetragonal Zirconia Translucent. *Dent Mater* **2014**, *30*, 1195–1203, doi:10.1016/j.dental.2014.08.375.
9. Srinivasan, R.; Angelis, R.D.; Davis, B.H. Factors Influencing the Stability of the Tetragonal Form of Zirconia. *Journal of Materials Research* **1986**, *1*, 583–588, doi:10.1557/JMR.1986.0583.

 doi:10.20944/preprints202508.1563.v1

10. Srinivasan, R.; Harris, M.B.; Simpson, S.F.; Angelis, R.J.D.; Davis, B.H. Zirconium Oxide Crystal Phase: The Role of the pH and Time to Attain the Final pH for Precipitation of the Hydrous Oxide. *Journal of Materials Research* **1988**, *3*, 787–797, doi:10.1557/JMR.1988.0787.
11. Li, Q.-L.; Jiang, Y.-Y.; Wei, Y.-R.; Swain, M.V.; Yao, M.-F.; Li, D.-S.; Wei, T.; Jian, Y.-T.; Zhao, K.; Wang, X.-D. The Influence of Yttria Content on the Microstructure, Phase Stability and Mechanical Properties of Dental Zirconia. *Ceramics International* **2022**, *48*, 5361–5368, doi:10.1016/j.ceramint.2021.11.079.
12. The Royal Society of Chemistry Available online: https://www.rsc.org/ (accessed on 10 August 2024).
13. Yoshida, M.; Hada, M.; Sakurada, O.; Morita, K. Transparent Tetragonal Zirconia Prepared by Sinter Forging at 950 °C. *Journal of the European Ceramic Society* **2023**, *43*, 2051–2056, doi:10.1016/j.jeurceramsoc.2022.12.031.
14. Xia, X. Computational Modelling Study of Yttria-Stabilized Zirconia.
15. Khanlari, K.; Shi, Q.; Li, K.; Hu, K.; Tan, C.; Zhang, W.; Cao, P.; Achouri, I.E.; Liu, X. Fabrication of Ni-Rich 58NiTi and 60NiTi from Elementally Blended Ni and Ti Powders by a Laser Powder Bed Fusion Technique: Their Printing, Homogenization and Densification. *Int J Mol Sci* **2022**, *23*, 9495, doi:10.3390/ijms23169495.
16. Daou, E.E. The Zirconia Ceramic: Strengths and Weaknesses. *TODENTJ* **2014**, *8*, 33–42, doi:10.2174/1874210601408010033.
17. Ahmed, W.M.; Troczynski, T.; McCullagh, A.P.; Wyatt, C.C.L.; Carvalho, R.M. The Influence of Altering Sintering Protocols on the Optical and Mechanical Properties of Zirconia: A Review. *J Esthet Restor Dent* **2019**, *31*, 423–430, doi:10.1111/jerd.12492.
18. Alshahrani, A.M.; Lim, C.H.; Wolff, M.S.; Janal, M.N.; Zhang, Y. Current Speed Sintering and High-Speed Sintering Protocols Compromise the Translucency but Not Strength of Yttria-Stabilized Zirconia. *Dental Materials* **2024**, *40*, 664–673, doi:10.1016/j.dental.2024.02.012.
19. Kaizer, M.R.; Gierthmuehlen, P.C.; dos Santos, M.B.; Cava, S.S.; Zhang, Y. Speed Sintering Translucent Zirconia for Chairside One-Visit Dental Restorations: Optical, Mechanical, and Wear Characteristics. *Ceramics International* **2017**, *43*, 10999–11005, doi:10.1016/j.ceramint.2017.05.141.
20. Paravina, R.; Ghinea, R.I.; Herrera, L.; Della Bona, A.; Igiel, C.; Linninger, M.; Sakai, M.; Takahashi, H.; Tashkandi, E.; Pérez Gómez, M. del M. Color Difference Thresholds in Dentistry. *Journal of Esthetic and Restorative Dentistry* **2015**, *27*, doi:10.1111/jerd.12149.
21. Rabel, K.; Blankenburg, A.; Steinberg, T.; Kohal, R.J.; Spies, B.C.; Adolfsson, E.; Witkowski, S.; Altmann, B. Gingival Fibroblast Response to (Hybrid) Ceramic Implant Reconstruction Surfaces Is Modulated by Biomaterial Type and Surface Treatment. *Dental Materials* **2024**, *40*, 689–699, doi:10.1016/j.dental.2024.02.018.
22. Chu, S. Color in Dentistry A Clinical Guide to Predictable Esthetics. *Stomatology Edu Journal* **2018**.
23. Halder, N.C.; Wagner, C.N.J. Separation of Particle Size and Lattice Strain in Integral Breadth Measurements. *Acta Cryst* **1966**, *20*, 312–313, doi:10.1107/S0365110X66000628.
24. SEC Available online: https://www.stevenabbott.co.uk/abbottapps/SEC/index.html (accessed on 14 August 2025).
25. Ghinea, R.; Pérez, M.M.; Herrera, L.J.; Rivas, M.J.; Yebra, A.; Paravina, R.D. Color Difference Thresholds in Dental Ceramics. *Journal of Dentistry* **2010**, *38*, e57–e64, doi:10.1016/j.jdent.2010.07.008.
26. Ebeid, K.; Wille, S.; Hamdy, A.; Salah, T.; El-Etreby, A.; Kern, M. Effect of Changes in Sintering Parameters on Monolithic Translucent Zirconia. *Dent Mater* **2014**, *30*, e419-424, doi:10.1016/j.dental.2014.09.003.
27. Pekkan, G.; Pekkan, K.; Bayindir, B.Ç.; Özcan, M.; Karasu, B. Factors Affecting the Translucency of Monolithic Zirconia Ceramics: A Review from Materials Science Perspective. *Dent Mater J* **2020**, *39*, 1–8, doi:10.4012/dmj.2019-098.
28. Kim, M.-J.; Ahn, J.-S.; Kim, J.-H.; Kim, H.-Y.; Kim, W.-C. Effects of the Sintering Conditions of Dental Zirconia Ceramics on the Grain Size and Translucency. *J Adv Prosthodont* **2013**, *5*, 161–166, doi:10.4047/jap.2013.5.2.161.
29. Yıldırım, B.; Recen, D. Color Stability and Translucency of Two CAD-CAM Restorative Materials Subjected To Mechanical Polishing, Staining, and Prophylactic Paste Polishing Procedures. *EÜ Dişhek Fak Derg* **2021**, *42*, 1–8, doi:10.5505/eudfd.2021.04127.

30. Kim, H.-K.; Kim, S.-H.; Lee, J.-B.; Han, J.-S.; Yeo, I.-S. Effect of Polishing and Glazing on the Color and Spectral Distribution of Monolithic Zirconia. *The Journal of Advanced Prosthodontics* **2013**, *5*, 296, doi:10.4047/jap.2013.5.3.296.
31. Kim, I.-J.; Lee, Y.-K.; Lim, B.-S.; Kim, C.-W. Effect of Surface Topography on the Color of Dental Porcelain. *Journal of Materials Science: Materials in Medicine* **2003**, *14*, 405–409, doi:10.1023/A:1023206716774.
32. Inokoshi, M.; Shimizu, H.; Nozaki, K.; Takagaki, T.; Yoshihara, K.; Nagaoka, N.; Zhang, F.; Vleugels, J.; Van Meerbeek, B.; Minakuchi, S. Crystallographic and Morphological Analysis of Sandblasted Highly Translucent Dental Zirconia. *Dental Materials* **2018**, *34*, 508–518, doi:10.1016/j.dental.2017.12.008.
33. Itoh, T.; Mori, M.; Inukai, M.; Nitani, H.; Yamamoto, T.; Miyanaga, T.; Igawa, N.; Kitamura, N.; Ishida, N.; Idemoto, Y. Effect of Annealing on Crystal and Local Structures of Doped Zirconia Using Experimental and Computational Methods. *Journal of Physical Chemistry C* **2015**, *119*, 8447–8458, doi:10.1021/jp5117118.
34. Belli, R.; Hurle, K.; Schürrlein, J.; Petschelt, A.; Werbach, K.; Peterlik, H.; Rabe, T.; Mieller, B.; Lohbauer, U. Relationships between Fracture Toughness, Y2O3 Fraction and Phases Content in Modern Dental Yttria-Doped Zirconias. *Journal of the European Ceramic Society* **2021**, *41*, 7771–7782, doi:10.1016/j.jeurceramsoc.2021.08.003.
35. Mayinger, F.; Ender, A.; Strickstrock, M.; Elsayed, A.; Nassary Zadeh, P.; Zimmermann, M.; Stawarczyk, B. Impact of the Sintering Parameters on the Grain Size, Crystal Phases, Translucency, Biaxial Flexural Strength, and Fracture Load of Zirconia Materials. *Journal of the Mechanical Behavior of Biomedical Materials* **2024**, *155*, 106580, doi:10.1016/j.jmbbm.2024.106580.
36. Scott, H.G. Phase Relationships in the Yttria-Rich Part of the Yttria-Zirconia System. *J Mater Sci* **1977**, *12*, 311–316, doi:10.1007/BF00566272.
37. Chevalier, J.; Gremillard, L.; Virkar, A.V.; Clarke, D.R. The Tetragonal-Monoclinic Transformation in Zirconia: Lessons Learned and Future Trends. *Journal of the American Ceramic Society* **2009**, *92*, 1901–1920, doi:10.1111/j.1551-2916.2009.03278.x.
38. Liu, H.; Inokoshi, M.; Nozaki, K.; Shimizubata, M.; Nakai, H.; Cho Too, T.D.; Minakuchi, S. Influence of High-Speed Sintering Protocols on Translucency, Mechanical Properties, Microstructure, Crystallography, and Low-Temperature Degradation of Highly Translucent Zirconia. *Dental Materials* **2022**, *38*, 451–468, doi:10.1016/j.dental.2021.12.028.
39. Qualitative X-ray Diffraction Analysis of Metastable Tetragonal (T′) Zirconia - Gibson - 2001 - Journal of the American Ceramic Society - Wiley Online Library Available online: https://ceramics.onlinelibrary.wiley.com/doi/abs/10.1111/j.1151-2916.2001.tb00708.x (accessed on 2 July 2025).
40. Yamashita, I.; Tsukuma, K. Phase Separation and Hydrothermal Degradation of 3 Mol% Y2O3-ZrO2 Ceramics. *J. Ceram. Soc. Japan* **2005**, *113*, 530–533, doi:10.2109/jcersj.113.530.
41. Alves, L.M.M.; Contreras, L.P.C.; Bueno, M.G.; Campos, T.M.B.; Bresciani, E.; Valera, M.C.; Melo, R.M. de The Wear Performance of Glazed and Polished Full Contour Zirconia. *Braz. Dent. J.* **2019**, *30*, 511–518, doi:https://doi.org/10.1590/0103-6440201902801.
42. Kim, Y.-S.; Shin ,Seung-Yun; Moon ,Seung-Kyun; and Yang, S.-M. Surface Properties Correlated with the Human Gingival Fibroblasts Attachment on Various Materials for Implant Abutments: A Multiple Regression Analysis. *Acta Odontologica Scandinavica* **2015**, *73*, 38–47, doi:10.3109/00016357.2014.949845.
43. Rutkunas, V.; Bukelskiene, V.; Sabaliauskas, V.; Balciunas, E.; Malinauskas, M.; Baltriukiene, D. Assessment of Human Gingival Fibroblast Interaction with Dental Implant Abutment Materials. *J Mater Sci: Mater Med* **2015**, *26*, 169, doi:10.1007/s10856-015-5481-8.
44. Lee, J.H.; Lee, S.J.; Khang, G.; Lee, H.B. The Effect of Fluid Shear Stress on Endothelial Cell Adhesiveness to Polymer Surfaces with Wettability Gradient. *Journal of Colloid and Interface Science* **2000**, *230*, 84–90, doi:10.1006/jcis.2000.7080.

 doi:10.20944/preprints202508.1563.v1

45. Lee, S.J.; Khang, G.; Lee, Y.M.; Lee, H.B. The Effect of Surface Wettability on Induction and Growth of Neurites from the PC-12 Cell on a Polymer Surface. *Journal of Colloid and Interface Science* **2003**, *259*, 228–235, doi:10.1016/S0021-9797(02)00163-7.
46. Mordanov, O.; Khabadze, Z.; Meremkulov, R.; Saeidyan, S.; Golovina, V.; Kozlova, Z.; Fokina, S.; Kostinskaya, M.; Eliseeva, T. EFFECT OF SURFACE TREATMENT PROTOCOLS OF ZIRCONIUM DIOXIDE MULTILAYER RESTORATIONS ON FUNCTIONAL PROPERTIES OF THE HUMAN ORAL MUCOSA STROMAL CELLS. *Georgian Med News* **2023**, 172–177.